

Design and Numerical Analysis of Ultra-High Negative Dispersion, Highly Birefringent Nonlinear Single Mode Core-Tune Photonic Crystal Fiber (CT-PCF) over Communication Bands

Amit Halder^{1,2*} , Wahiduzzaman Emon³, Md. Shamim Anower², Md. Riyad Tanshen¹, Md. Forkan¹, Md. Sharif Uddin Shajib¹

¹Department of Electrical and Electronic Engineering, World University of Bangladesh, Dhaka, Bangladesh

²Department of Electrical and Electronic Engineering, Rajshahi University of Engineering and Technology (RUET), Rajshahi, Bangladesh

³Department of Electrical and Electronic Engineering, Ahsanullah University of Science and Technology (AUST), Dhaka, Bangladesh

Email: *amit.rueten@gmail.com

How to cite this paper: Halder, A., Emon, W., Anower, Md.S., Tanshen, Md.R., Forkan, Md. and Shajib, Md.S.U. (2023) Design and Numerical Analysis of Ultra-High Negative Dispersion, Highly Birefringent Nonlinear Single Mode Core-Tune Photonic Crystal Fiber (CT-PCF) over Communication Bands. *Optics and Photonics Journal*, 13, 227-242.

<https://doi.org/10.4236/opj.2023.1310021>

Received: August 29, 2023

Accepted: October 10, 2023

Published: October 13, 2023

Copyright © 2023 by author(s) and Scientific Research Publishing Inc. This work is licensed under the Creative Commons Attribution-NonCommercial International License (CC BY-NC 4.0). <http://creativecommons.org/licenses/by-nc/4.0/>



Open Access

Abstract

This paper presents the development of a highly efficient CT-PCF (Core-Tune Photonic Crystal Fiber) with substantial birefringence, tailored for applications in high-bit-rate communication and sensing while minimizing signal loss. The design incorporates a modified broadband dispersion compensating structure, optimized for operation across the E, S, C, and L communication bands within a wavelength range spanning 1360 nm to 1625 nm. Notably, the CT-PCF demonstrates a remarkable birefringence of 2.372×10^{-2} at 1550 nm, surpassing traditional PCF structures. Single-mode performance is evaluated using the Higher Order Mode Extinction Ratio (HOMER) method, revealing a peak HOMER value of 10^4 at 1550 nm. Furthermore, at 1550 nm, the CT-PCF exhibits exceptional nonlinear characteristics, featuring a high nonlinearity of $50.74 \text{ W}^{-1} \cdot \text{Km}^{-1}$ for y polarization. In comparison to existing designs, the proposed CT-PCF exhibits superior performance metrics and optical characteristics. Additionally, the y polarization dispersion coefficient of the CT-PCF at 1550 nm is measured at $-3534 \text{ ps}/(\text{nm} \cdot \text{km})$. Overall, the CT-PCF represents a significant advancement, outperforming established systems in terms of performance metrics and optical properties.

Keywords

Negative Dispersion, Birefringence, Confinement Loss, HOMER Method, Single-Mode Performance, Optical Properties

1. Introduction

Optical fibers have evolved into an essential component for high-speed data transfer and other optical communication applications. However, ordinary optical fibers have dispersion and birefringence limits that might limit their performance in some applications. Photonic crystal fibers (PCFs) have emerged as a viable remedy to these restrictions. A periodic grid of air holes is present along the length of this optical cable [1]. The periodicity of air holes creates a photonic bandgap, which influences light propagation within the fiber and gives PCFs their specific characteristics. Hybrid PCFs are PCFs that combine the advantages of both traditional fibers and PCFs [2]. A typical fiber core is surrounded by a photonic crystal cladding in these fibers. The photonic crystal structure may be utilized to alter the dispersion properties of the fiber. Hybrid PCFs may achieve strong birefringence as well as negative dispersion, which is required for a wide range of optical communication system applications. Nevertheless, it is still challenging to attain both qualities at the same time since birefringence and dispersion are trade-offs. Researchers have been investigating several hybrid PCF architectures and designs in recent years in effort to overcome this trade-off and increase their performance. Previous research has introduced various PCF designs with high birefringence and negative dispersion coefficients. For instance, octagonal-shaped PCFs proposed by Habib *et al.* (2013) and Kaijage *et al.* (2009) have demonstrated negative dispersion factors of -588 and -239.51 ps/(nm·km) along with high birefringence values of 1.81×10^{-2} and 1.67×10^{-2} respectively [3] [4]. Similarly, spiral PCF designs have exhibited negative dispersion coefficients of -400 ps/(nm·km) and birefringence values of 1.6×10^{-2} [5]. However, these designs often come with limitations, such as costly manufacturing techniques or restricted operational wavelength ranges. To address these limitations, recent investigations have focused on enhancing PCF performance through innovative designs. One notable example is the use of elliptical air holes, as seen in a modified and defected core PCF, which achieved ultra-high birefringence (3.373×10^{-2}) and highly negative dispersion (-837.8 ps/(nm·km)) over a broad wavelength range, covering the E to L telecommunication bands [6]. Nevertheless, the manufacturing process for such PCFs can be intricate. Recent research efforts have also explored circular PCFs with defects, yielding birefringence values of 2.75×10^{-2} and negative dispersion coefficients of -331 ps/(nm·km) [7]. Other PCF designs have shown negative dispersion coefficients ranging from -134 to -385 ps/(nm·km) with birefringence values of 2.13×10^{-2} [8]. Additionally, a decagonal PCF achieved a negative dispersion of -390 ps/(nm·km) [9].

These advancements often incorporate elliptical air holes to enhance birefringence and negative dispersion coefficients. For example, Kim *et al.* proposed a defective core PCF with elliptical air holes, delivering a negative flattened dispersion of -1560.5 ps/(nm·km) and a birefringence of 1.94×10^{-2} [10]. Similarly, Ali *et al.* introduced a PCF with a circular cladding and an uneven core, achieving a birefringence of 2.78×10^{-2} and a negative dispersion of -345 ps/(nm·km) [11]. Furthermore, innovations like the modified square photonic crystal fiber (MS-PCF) design by Bikash Kumar Paul *et al.* have harnessed waveguide dispersion engineering to attain ultra-high negative dispersion while suppressing positive dispersion. The MS-PCF achieved an impressive negative dispersion of -2357.54 ps/nm/km, although it had a reduced birefringence of 1.42×10^{-5} and a relatively high confinement loss of 898.75 dB/km [12]. In a separate study, Pandey *et al.* introduced a dispersion compensating hexagonal photonic crystal fiber (DC-HPCF) featuring circular air holes in the cladding zone. This fiber design integrated a rectangular slot filled with Gallium phosphide (GaP) within the core area, optimizing key optical parameters. At 1.55 μm , the DC-HPCF exhibited substantial negative dispersion (-2885 ps/(nm·km)) and notable birefringence (0.121), making it suitable for applications like four-wave mixing, polarization splitting, polarization-maintaining fiber, and dispersion compensation [13].

Our work introduces a highly efficient Core-Tune Photonic Crystal Fiber (CT-PCF) design that achieves exceptional birefringence, surpassing conventional PCF structures, with a remarkable value of 2.372×10^{-2} at 1550 nm. This birefringence is crucial for polarization-maintaining transmission, enhancing signal integrity in high-bit-rate data transfer. Additionally, our CT-PCF demonstrates outstanding single-mode performance, as indicated by a peak Higher Order Mode Extinction Ratio (HOMER) value of 10^4 at 1550 nm, making it ideal for high-bit-rate communication systems. Furthermore, our CT-PCF exhibits exceptional nonlinear characteristics with a high nonlinearity of 50.74 $\text{W}^{-1}\cdot\text{Km}^{-1}$ for y polarization, making it promising for advanced optical devices. Our research introduces a novel modified Core Tune Photonic Crystal Fiber (CT-PCF) that simultaneously overcomes the traditional trade-off between birefringence and dispersion, offering a breakthrough in optical fiber design, while also simplifying manufacturing for cost-effective high-performance optical communication systems. In summary, our CT-PCF represents a significant advancement in optical fiber technology, outperforming existing designs in birefringence, single-mode performance, and nonlinear characteristics, thus offering great potential for high-bit-rate communication and sensing applications.

2. Geometry of Proposed CT-PCF Structure

The Core-Tune Photonic Crystal Fiber (CT-PCF) incorporates a distinct design for its fiber cladding, which comprises circular air holes running along its length. In the cross-sectional view presented in **Figure 1**, the core of the CT-PCF has been deliberately modified to introduce two hexagonal rings in the inner cladding

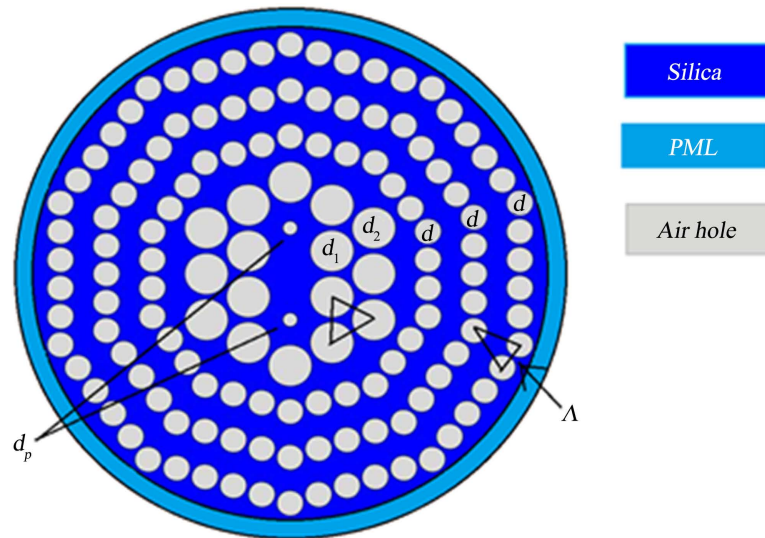


Figure 1. In the transverse cross-sectional perspective of the envisioned CT-PCF design, the pitch (Λ) is set at $0.9 \mu\text{m}$, with a ratio of the smaller air hole diameter (d_p) to Λ equal to 0.3. The first and second ring air hole diameters (d_1 and d_2) are both 0.9 times Λ , and the diameter (d) of the air holes in the third ring is 0.55 times Λ .

layer and three decagonal rings in the outer cladding layer. Furthermore, the cladding includes five concentric rings of air holes. To enhance its effectiveness, adjustments were made to the inner core by adding two smaller air holes to the initial ring of air holes, while leaving the other four air holes unaltered from the original six. This design adaptation was aimed at optimizing both birefringence and dispersion stability, given that these characteristics were primarily influenced by the two smaller air holes in the initial ring. To additionally minimize the loss of light confinement within the fiber, five circular air hole rings were integrated into the CT-PCF setup. It's worth noting that the flawed core ring within the cladding configuration was strategically employed to amplify birefringence. The critical dimensions consist of a diameter (d_p) of $0.27 \mu\text{m}$ for the smaller air holes, and identical diameters ($d_1 = d_2 = 0.81 \mu\text{m}$) for the air holes in the first and second ring of the hexagonal structure. The third through fifth air holes in the decagonal structure have a diameter (d) of $0.495 \mu\text{m}$. The pitch (Λ) in the CT-PCF signifies the spacing between air holes within two consecutive rings. In essence, the configuration of the Core-Tune PCF (CT-PCF) presents a well-considered arrangement of air holes within the cladding and core, effectively optimizing birefringence, dispersion stability, and light confinement loss to attain enhanced performance across various applications.

3. Computational Methodology

The optical characteristics of the CT-PCF structures were examined through finite element method (FEM) simulations, and the results were assessed utilizing the COMSOL Multiphysics software. The finite element technique with perfectly matched layers (PML) boundary conditions was employed to compute attributes

such as chromatic dispersion, effective area, and confinement loss of the proposed microstructured optical fibers (MOFs). Modal properties of the fiber were computed using a commercial full-vector finite-element software (COMSOL) with first-order triangular vector edge elements. The simulation incorporated the Sellmeier equation to determine the refractive index of silica, accounting for its wavelength dependence. By solving an eigenvalue problem, FEM yielded the modal effective index (n_{eff}), which subsequently enabled the calculation of parameters like chromatic dispersion ($D(\lambda)$), birefringence and confinement loss using the provided equations [14].

$$D(\lambda) = -\frac{\lambda}{c} \times \frac{d^2 \text{Re}[n_{eff}]}{d\lambda^2} \quad (1)$$

$$L_c = 8.686 \times \frac{2\pi f}{c} \times \text{Im}[n_{eff}] \quad (2)$$

$$B = |n_{eff,x} - n_{eff,y}| \quad (3)$$

The higher order mode extinction ratio (HOMER) is a measurement of the power ratio in a photonic crystal fiber (PCF) between the basic mode and higher order modes [15]. Equation (4) is used to obtain the number that describes the single-mode performance of a Core-Tune photonic crystal fiber.

$$\text{HOMER} = \frac{\min(CL_{HOM})}{CL_{FM}} \quad (4)$$

where, CL_{HOM} is the basic mode confinement loss and CL_{FM} is the higher-order mode confinement loss.

The effective area A_{eff} is calculated using Equation (5) as follows [16]:

$$A_{eff} = \frac{\left(\iint |E|^2 dx dy \right)^2}{\iint |E|^4 dx dy} \quad (5)$$

A_{eff} is quantified in square micrometers (μm^2) and maintains a proportional relationship with the electric field's amplitude, denoted as E , within the medium. Consequently, comprehending the nonlinear phenomena taking place within photonic crystal fibers (PCFs) demands a thorough grasp of A_{eff} . The correlation between the Kerr constant (representing the nonlinear refractive index coefficient), n_2 , and the effective mode area at a specific optical field wavelength serves as a crucial gauge for evaluating the magnitude of nonlinear effects. This nonlinear coefficient, which aligns with the effective mode area, can be computed employing the subsequent formula [17]:

$$\gamma = \frac{2\pi n_2}{\lambda A_{eff}} \quad (6)$$

4. Numerical Analysis Outcomes and Discussion

4.1. Chromatic Dispersion

Figure 2 illustrates the dispersion characteristics for both x and y polarizations,

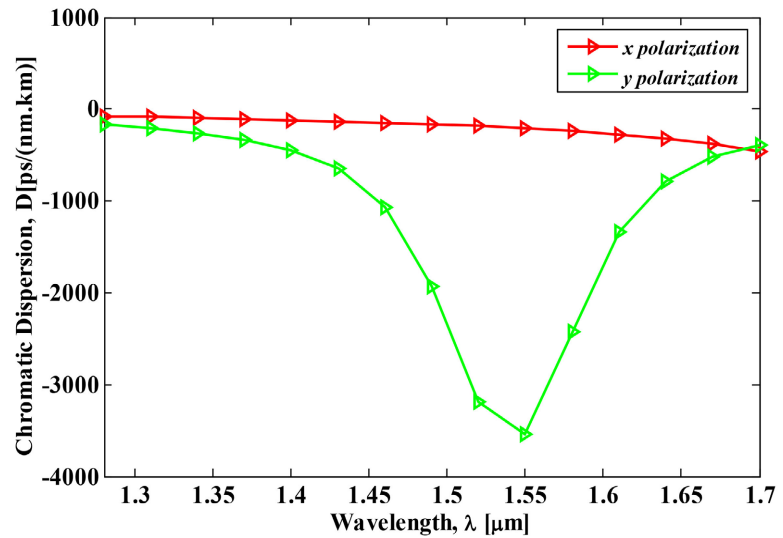


Figure 2. The wavelength-specific dispersion curves of the suggested CT-PCF for x and y polarizations are depicted.

utilizing the optimized design parameters: $d/\Lambda = 0.55$, $d_p/\Lambda = 0.3$, $d_1/\Lambda = d_2/\Lambda = 0.9$, and a pitch $\Lambda = 0.9$ μm for the hexagonal cladding arrangement. Within this cladding structure, the initial ring of smaller air holes possesses an overall diameter $d_p/\Lambda = 0.3$, while the remaining air holes in the first and second rings share an overall diameter of $d_1/\Lambda = d_2/\Lambda = 0.9$. In the decagonal ring structure, the diameter parameter spans $d/\Lambda = 0.55$ for the third through fifth air hole rings. At a wavelength of 1550 nm, the dispersion curve concerning wavelength showcases a negative dispersion coefficient of -211 ps/(nm.km) for x polarization. Examining the wavelength-dispersion graph, it's evident that the proposed CT-PCF exhibits a remarkably high negative dispersion coefficient for y polarization at 1550 nm, specifically around -3534 ps/(nm.km). This negative y polarization dispersion value stands out as the most prominent dispersion outcome within this experiment. Given its substantial negative dispersion coefficient, these suggested CT-PCFs emerge as strong contenders for addressing dispersion issues in high-bit-rate transmission networks.

During the fabrication of PCFs, there is the potential for a $\pm 1\%$ fluctuation in the overall diameters of the structure. With this consideration in mind, we conducted an assessment to understand the impact of these variations on dispersion and birefringence, exploring changes spanning from $\pm 1\%$ to $\pm 2\%$. As depicted in **Figure 3**, we focused on the influence of adjusting the global pitch width while keeping other parameters constant. In the graph, the solid line signifies parameter increments, while the dotted line signifies parameter reductions. The resulting CT-PCF dispersion values for pitch adjustments ranging from $\pm 1\%$ to $\pm 2\%$ are approximately -3675 , -3605 , -3463 , and -3393 ps/(nm.km). For long-distance optical communication, a PCF with remarkably high negative dispersion is desirable, as it leads to minimal pulse broadening and spreading. Despite the existence of negative dispersion PCF models, there remain gaps in their development.

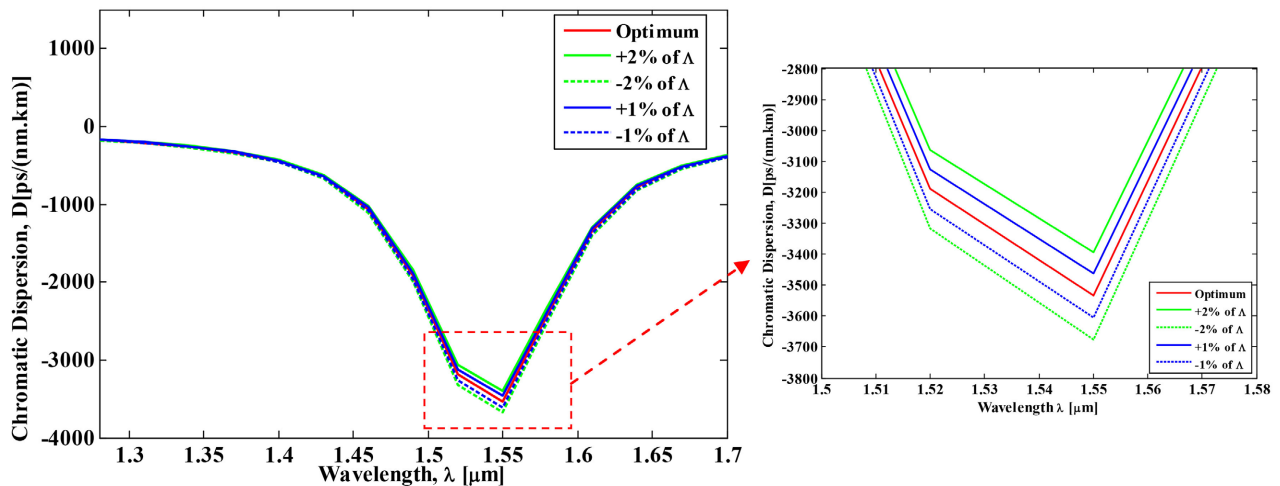


Figure 3. The effect of adjusting the pitch value of the proposed CT-PCF on dispersion vs. wavelength with partial enlargement view.

To fulfill the requirements for dispersion profiles in optical communication, the strong recommendation is to pursue configurations with ultra-high negative dispersion.

4.2. Birefringence

The capacity to retain polarization is mirrored by fiber birefringence, which is a crucial feature for enhancing system accuracy and stability, particularly in sensing applications. The birefringence feature of the recommended CT-PCF designs is seen in **Figure 4**, which has a strong birefringence due to its uneven core design. Normal polarization preserving fibers have a modal birefringence of around 5×10^{-4} [18], while the proposed CT-PCF design may achieve a display birefringence of about 2.372×10^{-2} , making it an appealing candidate for sensing applications. **Figure 4** additionally demonstrates how pitch affects CT-PCF birefringence, which varies by 0.02324, 0.02348, 0.02395, and 0.02419, respectively, whereas pitch changes by $\pm 1\%$ to $\pm 2\%$ at 1550 nm. The proposed high birefringence CT-PCF has applications in optical fiber communications, fiber lasers, and fiber sensors, as well as nonlinear optical applications where the extra negative dispersion characteristic may be used as a chromatic dispersion controller or to compensate for dispersion.

4.3. Single Mode Performance Analysis

Because optical fibers can support higher-order modes (HOMs), this section examines the performance of our proposed CT-PCF fiber in the context of single-mode operation. In cases where the losses in these higher-order modes significantly surpass the losses in the fundamental mode (FM), the fiber can effectively function as a single-mode fiber. To assess this, we calculate the higher order mode extinction ratio (HOMER), which gauges the light leakage loss associated with the higher-order modes, as opposed to that of the fundamental

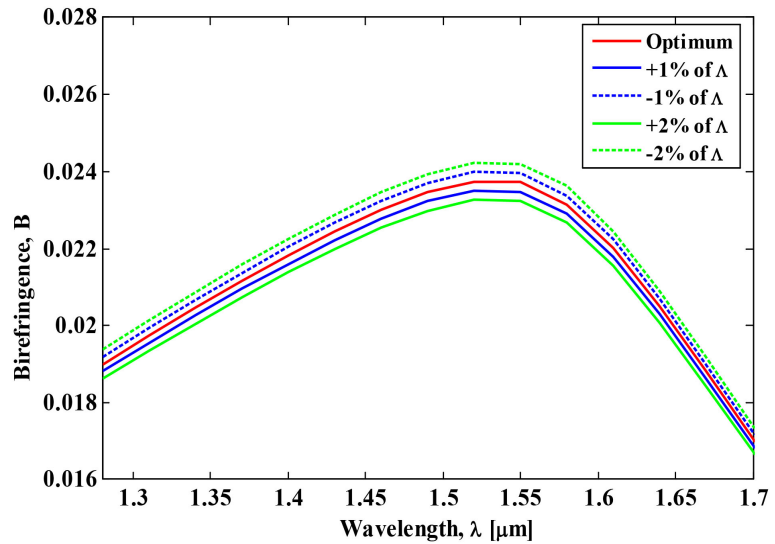
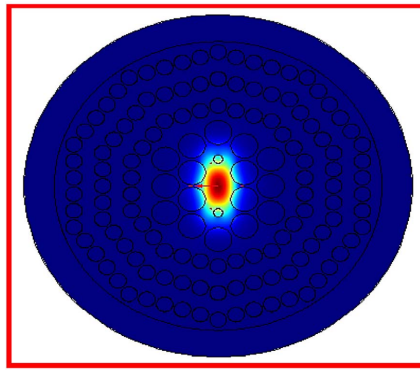


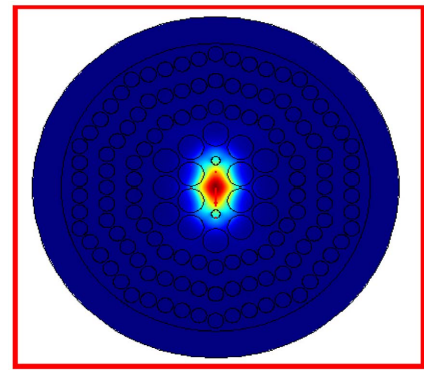
Figure 4. A plot depicting the relationship between wavelength and birefringence for the CT-PCF under optimal design parameters is shown, considering variations in pitch within the range of $\pm 1\%$ to $\pm 2\%$.

mode's leakage loss. Among the initial six core modes, including both fundamental and higher-order modes, are HE_{11} , HE_{21} , HE_{31} , TE_{01} , TM_{01} , and EH_{11} . **Figure 5** illustrates the spatial distribution of various higher-order modes under investigation for both x and y polarization scenarios.

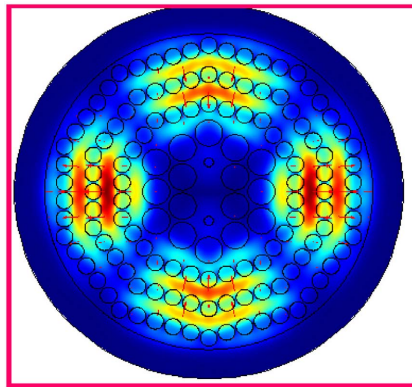
In **Figure 6(a)**, the confinement loss for x polarization of the first six core modes in the CT-PCF is portrayed concerning wavelength. Operating at 1550 nm, the fundamental modes, such as HE_{11} , exhibit a loss of 3.07×10^{-6} dB/m. For the same wavelength, higher-order modes (HOMs) like TE_{01} , TM_{01} , HE_{21} , EH_{11} , and HE_{31} demonstrate losses of 4.66×10^{-2} , 2.884×10^{-3} , 5.802×10^{-3} , 3.717×10^{-3} , and 8.405×10^{-3} dB/m, respectively. Within the transmission band at 1550 nm, TM_{01} is highlighted for having lower losses among the higher-order modes. Furthermore, while the fundamental mode loss elevates across the O, E, S, C and L communication bands from 10^{-8} to 10^{-5} order ranges, the HOMs vary within the 10^{-3} to 10^{-2} order ranges. Examining **Figure 6(b)**, it's observed that the highest HOMER of the CT-PCF at 1550 nm operating wavelength is approximately 10^4 , consistently maintaining values greater than 100 throughout the communication windows. In **Figure 7(a)**, the confinement loss for y polarization of the first six core modes in the CT-PCF is depicted as a function of wavelength. Operating at 1550 nm, the fundamental mode HE_{11} encounters a loss of 3.957×10^{-4} dB/m. At the same working wavelength, the HOMs exhibit losses of 4.66×10^{-2} , 2.884×10^{-3} , 5.084×10^{-3} , 2.67×10^{-3} , and 9.786×10^{-3} dB/m, respectively. When investigating losses at the communication-appropriate wavelength of 1550 nm, EH_{11} stands out with lower loss among the higher-order modes. In the O to L communication bands, the HOMs show losses varying from the 10^{-3} to 10^{-2} order ranges, whereas the fundamental mode loss increases from 10^{-7} to 10^{-3} order ranges. The overarching aim is to sustain an HOMER of



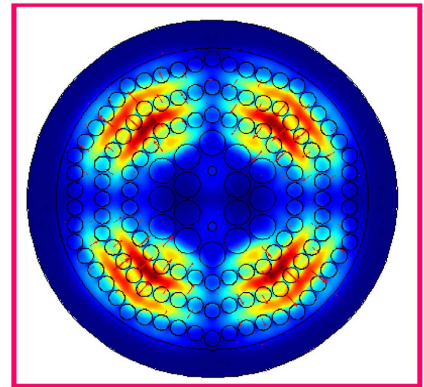
(a)



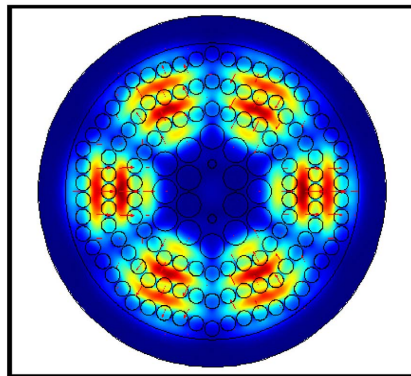
(b)



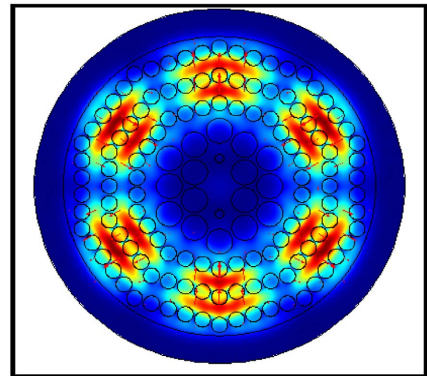
(c)



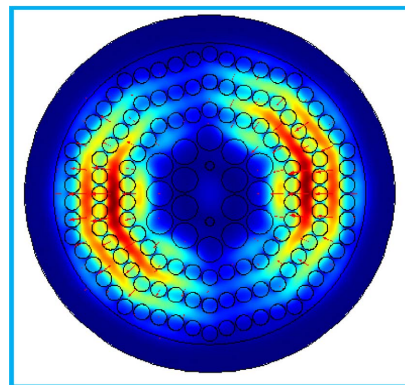
(d)



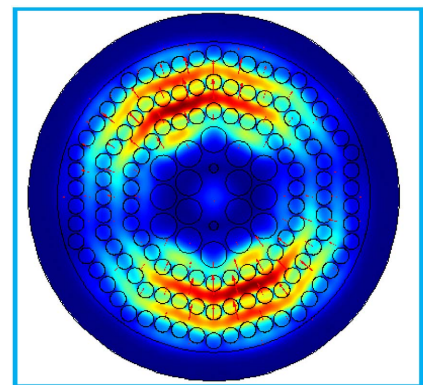
(e)



(f)



(g)



(h)

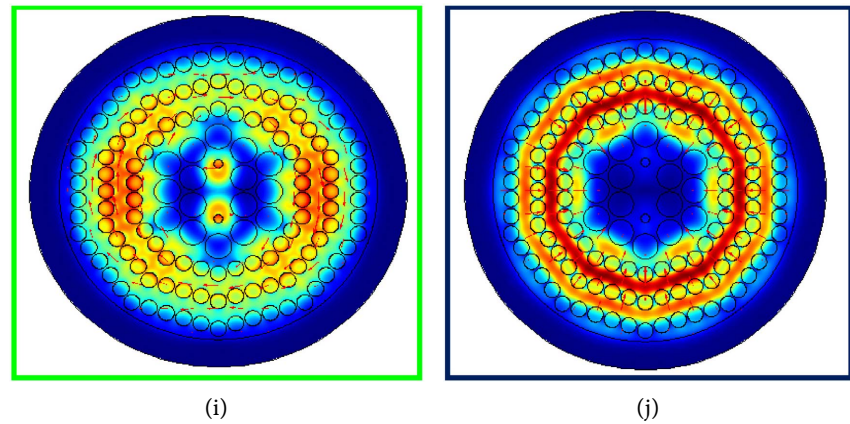
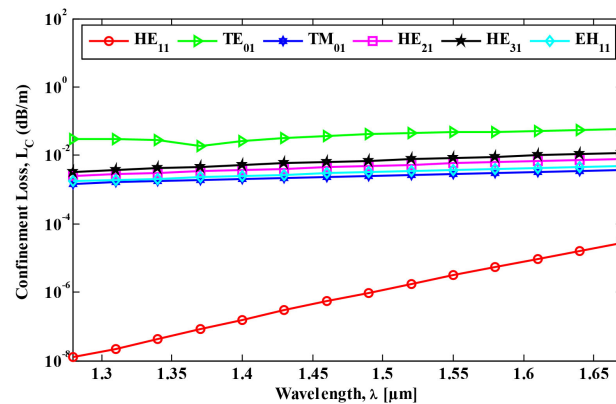
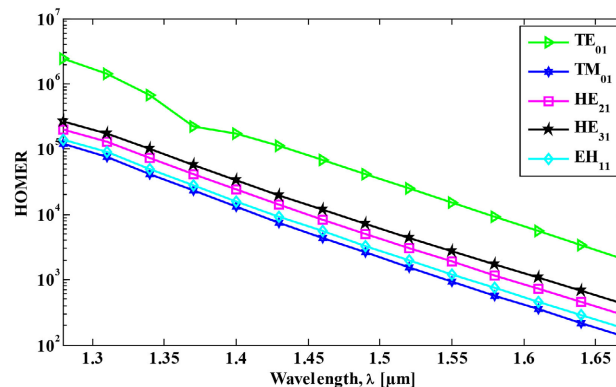


Figure 5. Fundamental and higher order modes (HOMs) field distribution with its directions for proposed CT-PCF. (a) HE₁₁ x-polarization; (b) HE₁₁ y-polarization; (c) HE₂₁ x-polarization; (d) HE₂₁ y-polarization; (e) HE₃₁ x-polarization; (f) HE₃₁ y-polarization; (g) EH₁₁ x-polarization; (h) EH₁₁ y-polarization; (i) TE₀₁ for both polarization; (j) TM₀₁ for both polarization.

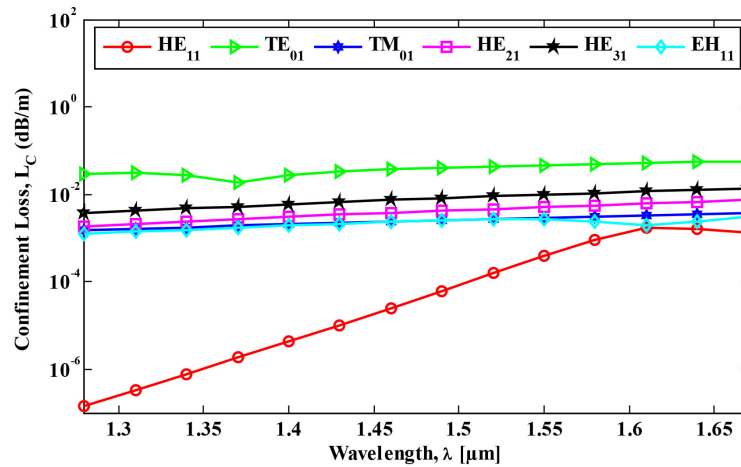


(a)

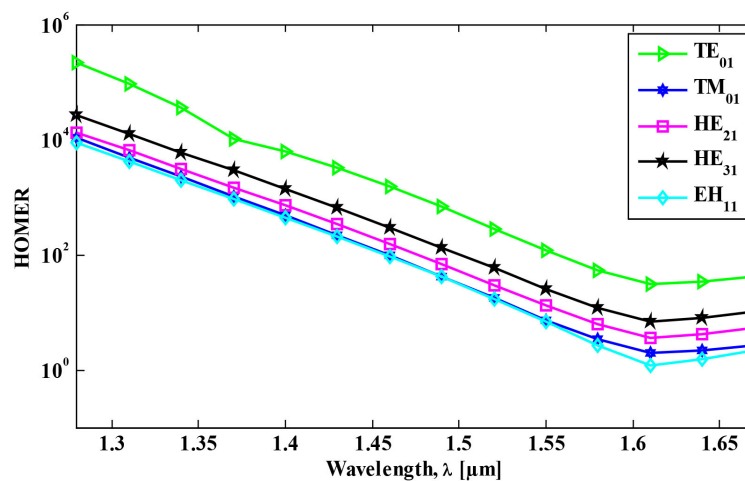


(b)

Figure 6. (a) The loss characteristics of the CT-PCF under consideration are studied with respect to wavelength, encompassing both fundamental and higher-order modes (HOMs). (b) The higher-order mode extinction ratio (HOMER) of the CT-PCF for x polarization is examined across varying wavelengths. Notably, TM₀₁ emerges as the HOM with the least loss in this scenario. In **Figure 5**, the color of each frame depicting the modes in x polarization corresponds to the color of the loss curve's lines.



(a)



(b)

Figure 7. (a) The CT-PCF's loss characteristics, encompassing both fundamental and higher-order modes (HOMs), are examined in relation to wavelength. (b) The higher-order mode extinction ratio (HOMER) of the CT-PCF is evaluated for y polarization across a range of wavelengths. It is worth noting that EH11 exhibits the lowest loss among the higher-order modes in this instance. In **Figure 5**, the color of each frame illustrating the modes in y polarization corresponds to the color of the lines in the loss curve.

at least 10 over a wide bandwidth to ensure robust single-mode performance. The proposed CT-PCF approach strives for the highest achievable HOMER across an extensive range of wavelengths. As portrayed in **Figure 7(b)**, the maximum HOMER for CT-PCF at the 1550 nm operating wavelength is about 10^2 , maintaining values exceeding 10 throughout both communication windows.

4.4. Effective Area and Nonlinearity

Figure 8 shows the greatest effective area values for the CT-PCF for x and y polarization at 1550 nm, which are $2.657 \mu\text{m}^2$ and $2.397 \mu\text{m}^2$, respectively. **Figure 9** depicts the nonlinearity curve of the disclosed CT-PCF at optimal pitch of the design parameters.

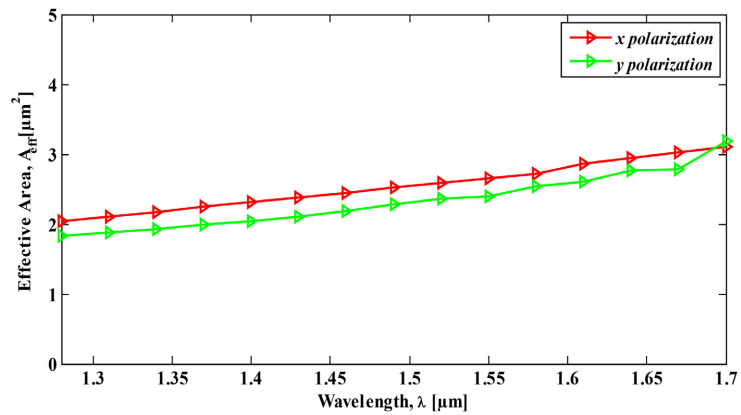


Figure 8. The graph depicting the effective area in relation to wavelength for the proposed CT-PCF under optimal design parameters is shown separately for both x and y polarizations.

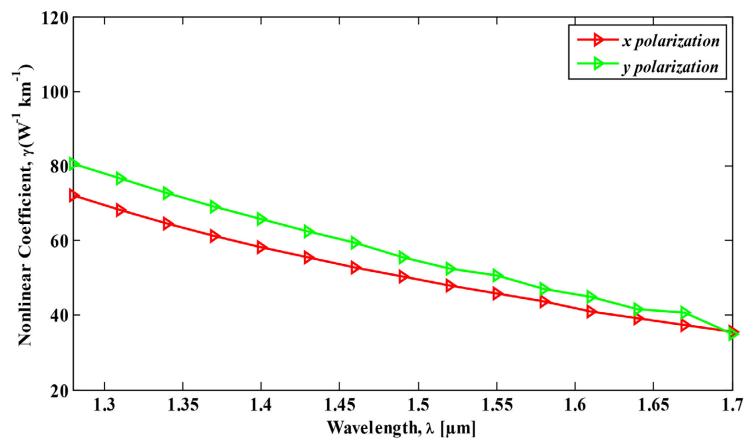


Figure 9. The curve illustrating the nonlinear coefficient in relation to wavelength for the recommended CT-PCF under optimal design parameters is presented for both x and y polarizations.

At a wavelength of 1550 nm, the nonlinearity values were recorded as $45.77 \text{ W}^{-1} \cdot \text{km}^{-1}$ for x polarization and $50.74 \text{ W}^{-1} \cdot \text{km}^{-1}$ for y polarization, as shown in **Figure 9**. The outcomes demonstrate that the suggested design of the CT-PCF offers favorable characteristics in terms of effective area and nonlinearity, making it suitable for applications involving nonlinear effects.

4.5. Confinement Loss

Confinement losses are caused by the leaky nature of modes and faults in the design of a PCF fiber. These losses lead to a loss that varies with wavelength, influencing the mode propagation. This modulation is controlled by factors such as the count of air hole rings and the dimensions of the air holes within the fiber structure. The confinement loss in the O to L telecommunication bands varies from 10^{-8} to 10^{-2} order, which is relatively low for this wavelength range. **Figure 10** displays the proposed CT-PCF fiber's wavelength-dependent confinement loss.

The optimal confinement loss value of CT-PCF x and y polarizations at the working wavelength 1550 nm is 3.07×10^{-6} and 3.957×10^{-4} dB/m, respectively. The graph clearly shows that the confinement loss increases as the wavelength increases. This graph trend demonstrated that as the fundamental field distribution of the recommended PCFs increased with respect to wavelength, so did the leaky nature of the mode. The same logic applies to the fact that x polarization has a smaller confinement loss than y polarization. **Table 1** compares the parameters of the proposed CT-PCF to those of earlier PCF waveguides at 1550 nm.

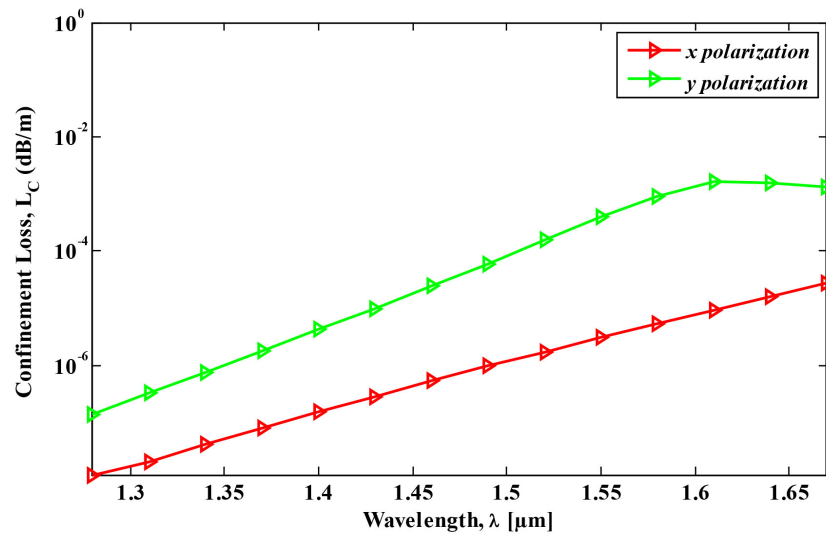


Figure 10. The graph portraying the relationship between confinement loss and wavelength, employing the optimal design parameters, is shown separately for x and y polarizations in the CT-PCF.

Table 1. Modal property comparisons of the proposed CT-PCF and other designs.

Prior references	Cladding structure	Dispersion $D(\lambda)$ [ps/(nm·km)]	Birefringence, $B = n_x - n_y $	Confinement loss, L_c (dB/m)
Ref. [3]	Octagonal	-588	1.81×10^{-2}	<10
Ref. [4]	Octagonal	-239.51	1.67×10^{-2}	3.2×10^{-5}
Ref. [5]	Spiral	-400	1.60×10^{-2}	-
Ref. [7]	Defected core circular	-331	2.75×10^{-2}	-
Ref. [8]	Square-core octagonal	-294.1	2.13×10^{-2}	0.42
Ref. [10]	Elliptical air hole hexagonal	-156 ± 0.5	1.94×10^{-2}	10^{-4}
Ref. [11]	Asymmetric core circular	-345	2.78×10^{-2}	< 10^{-2}
Ref. [12]	Modified square shape	-2357.54	1.42×10^{-5}	0.89875
Ref. [13]	Hexagonal	-2885	0.121	-
Proposed CT-PCF	Defected core hybrid (Hexagonal-decagonal)	-3534	2.372×10^{-2}	3.071×10^{-6}

5. Conclusion

This study successfully demonstrates the creation of a Core-Tune photonic crystal fiber (CT-PCF) with notably high birefringence and substantial negative dispersion. Employing a modified broadband dispersion compensating structure, the CT-PCF functions effectively across the O to L telecommunication bands, spanning wavelengths from 1280 nm to 1790 nm. Specifically, at an operating wavelength of 1550 nm, the proposed CT-PCF design achieves an elevated birefringence value of 2.372×10^{-2} , surpassing conventional PCF structures. For assessing the single-mode performance of CT-PCF, the Higher Order Mode Extinction Ratio (HOMER) method is employed. Remarkably, the CT-PCF records a maximum HOMER value of 10^4 at 1550 nm, attesting to its single-mode proficiency. In terms of dispersion properties, the CT-PCF exhibits a y polarization dispersion coefficient of -3534 ps/(nm·km) at 1550 nm, alongside a notably high nonlinear coefficient of 50.74 W⁻¹·km⁻¹. The suggested CT-PCF stands out by excelling in performance metrics and optical attributes when compared to existing systems. With an impressively low confinement loss of 3.071×10^{-6} dB/m across the broadband communication bands, the proposed CT-PCF emerges as an ideal candidate for diverse applications, encompassing sensing and high-bit-rate transmission, offering minimal signal degradation. As we reflect on the limitations of this study, it is important to acknowledge that while our CT-PCF design represents a significant advancement, further research is needed to explore its practical implementation and scalability. The fabrication and deployment of such specialized fibers may pose challenges that need to be addressed in future investigations. Additionally, the integration of our CT-PCF into real-world communication systems and its performance under various environmental conditions warrant further exploration. Finally, our research gives us new avenues for the creation of high-performance optical fibers with a wide variety of applications.

Acknowledgements

Authors of this manuscript are grateful to the support of Photonics Simulation Lab of World University of Bangladesh, Dhaka-1230, Bangladesh.

Conflicts of Interest

The authors declare no conflicts of interest regarding the publication of this paper.

References

- [1] Zolla, F., Renversez, G., Nicolet, A., Kuhlmeiy, B., Guenneau, S.R. and Felbacq, D. (2005) Foundations of Photonic Crystal Fibres. World Scientific, Singapore, 376. <https://doi.org/10.1142/p367>
- [2] Markos, C., Travers, J.C., Abdolvand, A., Eggleton, B.J. and Bang, O. (2017) Hybrid Photonic-Crystal Fiber. *Reviews of Modern Physics*, **89**, Article ID: 045003.

- <https://doi.org/10.1103/RevModPhys.89.045003>
- [3] Habib, M.S., Habib, M.S., Razzak, S.A. and Hossain, M.A. (2013) Proposal for Highly Birefringent Broadband Dispersion Compensating Octagonal Photonic Crystal Fiber. *Optical Fiber Technology*, **19**, 461-467. <https://doi.org/10.1016/j.yofte.2013.05.014>
- [4] Kaijage, S.F., Namihira, Y., Hai, N.H., Begum, F., Razzak, S.A., Kinjo, T., Miyagi, K. and Zou, N. (2009) Broadband Dispersion Compensating Octagonal Photonic Crystal Fiber for Optical Communication Applications. *Japanese Journal of Applied Physics*, **48**, Article ID 052401. <https://doi.org/10.1143/JJAP.48.052401>
- [5] Agrawal, A., Kejalakshmy, N., Chen, J., Rahman, B.M.A. and Grattan, K.T.V. (2008) Golden Spiral Photonic Crystal Fiber: Polarization and Dispersion Properties. *Optics Letters*, **3**, 2716-2718. <https://doi.org/10.1364/OL.33.002716>
- [6] Halder, A. (2016) Highly Birefringent Photonic Crystal Fiber for Dispersion Compensation over E + S + C + L Communication Bands. 2016 5th International Conference on Informatics, Electronics and Vision (ICIEV), Dhaka, 13-14 May 2016, 1099-1103. <https://doi.org/10.1109/ICIEV.2016.7760169>
- [7] Ali, M.S., Nasim, K.M., Ahmad, R., Khan, M.A.G. and Habib, M.S. (2013) A Defected Core Highly Birefringent Dispersion Compensating Photonic Crystal Fiber. 2013 2nd International Conference on Advances in Electrical Engineering (ICAEE), Dhaka, 19-21 December 2013, 100-105. <https://doi.org/10.1109/ICAEE.2013.6750313>
- [8] Habib, M.S., Rana, M.S., Moniruzzaman, M., Ali, M.S. and Ahmed, N. (2014) Highly Birefringent Broadband-Dispersion-Compensating Photonic Crystal Fibre over the E + S + C + L + U Wavelength Bands. *Optical Fiber Technology*, **20**, 527-532. <https://doi.org/10.1016/j.yofte.2014.06.004>
- [9] Islam, M.A., Ahmad, R., Ali, M.S. and Nasim, K.M. (2014) Proposal for Highly Residual Dispersion Compensating Defected Core Decagonal Photonic Crystal Fiber over S + C + L + U Wavelength Bands. *Optical Engineering*, **53**, Article ID: 076106. <https://doi.org/10.1117/1.OE.53.7.076106>
- [10] Kim, S.E., Kim, B.H., Lee, C.G., Lee, S., Oh, K. and Kee, C.S. (2012) Elliptical Defected Core Photonic Crystal Fiber with High Birefringence and Negative Flattened Dispersion. *Optics Express*, **20**, 1385-1391. <https://doi.org/10.1364/OE.20.001385>
- [11] Ali, S., Ahmed, N., Islam, M., Aljunid, S.A., Ahmed, B.B., Hussain, S. and Rahman, E. (2016) A High Birefringent PCF with RDS Matched Dispersion Compensation over S + C + L Communication Bands. 2016 3rd International Conference on Electronic Design (ICED), Phuket, 11-12 August 2016, 136-140. <https://doi.org/10.1109/ICED.2016.7804623>
- [12] Paul, B.K., Ahmed, K., Rani, M.T., Pradeep, K.S. and Al-Zahrani, F.A. (2022) Ultra-High Negative Dispersion Compensating Modified Square Shape Photonic Crystal Fiber for Optical Broadband Communication. *Alexandria Engineering Journal*, **61**, 2799-2806. <https://doi.org/10.1016/j.aej.2021.08.006>
- [13] Pandey, S.K., Dwivedi, P., Singh, S. and Prajapati, Y.K. (2022) Design of a Dispersion Compensating Hexagonal Photonic Crystal Fiber (DC-HPCF) for High Nonlinearity and Birefringence. In: Angrisani, L., Arteaga, M.A., Chakraborty, S., et al., Eds. *Advances in VLSI, Communication, and Signal Processing: Select Proceedings of VCAS2021*, Springer Nature Singapore, Singapore, 187-199. https://doi.org/10.1007/978-981-19-2631-0_17
- [14] Agrawal, G.P. (2004) *Lightwave Technology: Components and Devices* (Vol. 1). John Wiley & Sons, Hoboken.

- [15] Gu, S., Wang, X., Jia, H., Xing, Z. and Lou, S. (2022) Single-Mode Bend-Resistant Hollow-Core Fiber with Multi-Size Anti-Resonant Elements. *Infrared Physics & Technology*, **123**, Article ID: 104159. <https://doi.org/10.1016/j.infrared.2022.104159>
- [16] Guo, S., Wu, F., Albin, S., Tai, H. and Rogowski, R.S. (2004) Loss and Dispersion Analysis of Microstructured Fibers by Finite-Difference Method. *Optics Express*, **12**, 3341-3352. <https://doi.org/10.1364/OPEX.12.003341>
- [17] Poli, F., Cucinotta, A., Selleri, S. and Bouk, A.H. (2004) Tailoring of Flattened Dispersion in Highly Nonlinear Photonic Crystal Fibers. *IEEE Photonics Technology Letters*, **16**, 1065-1067. <https://doi.org/10.1109/LPT.2004.824624>
- [18] Piliarik, M., Homola, J., Maniková, Z. and Čtyroký, J. (2003) Surface Plasmon Resonance Sensor Based on a Single-Mode Polarization-Maintaining Optical Fiber. *Sensors and Actuators B: Chemical*, **90**, 236-242. [https://doi.org/10.1016/S0925-4005\(03\)00034-0](https://doi.org/10.1016/S0925-4005(03)00034-0)